

## Gene expression in the deep biosphere

William D. Orsi<sup>1\*</sup>, Virginia P. Edgcomb<sup>1</sup>, Glenn D. Christman<sup>2</sup>, and Jennifer F. Biddle<sup>2</sup>

Affiliations:

<sup>1</sup> Department of Geology and Geophysics, Woods Hole Oceanographic Institution

<sup>2</sup> College of Earth, Ocean, and Environment, University of Delaware

Keywords: marine subsurface, mRNA, metatranscriptomics, deep biosphere, Illumina sequencing, marine sediment, seafloor, ODP Leg 201, gene expression

Running title: Gene expression in the deep biosphere.

\*To whom correspondence should be addressed

**Scientific ocean drilling has revealed a deep biosphere of widespread microbial life in sub-seafloor sediment. Microbial metabolism in the marine subsurface likely plays an important role in global biogeochemical cycles<sup>1-3</sup> but deep biosphere activities are not well understood<sup>1</sup>. Here, we describe and analyze the first subseafloor metatranscriptomes from anaerobic Peru Margin sediment up to 159 meters below seafloor (mbsf) represented by over 1 billion cDNA sequence reads. Anaerobic metabolism of amino acids, carbohydrates, and lipids appear to be dominant metabolic processes, and profiles of dissimilatory sulfite reductase (*Dsr*) transcripts are consistent with porewater sulfate concentration profiles<sup>1</sup>. Moreover, transcripts involved in cell division increase as a function of microbial cell concentration, indicating that increases in subseafloor microbial abundance are a function**

24 **of cell division across all three domains of life. These data support calculations<sup>1</sup> and**  
25 **models<sup>4</sup> of subseafloor microbial metabolism and represent the first holistic picture of deep**  
26 **biosphere activities.**

27 Abundant microbial cells<sup>5, 6</sup> exist in sub-seafloor (>1.5 mbsf) sediment and represent a  
28 significant portion of Earth's biomass<sup>7, 8</sup>. Marine sediment contains Earth's largest pool of  
29 organic carbon, which may be the primary energy source for subsurface microbes<sup>1, 2, 9, 10, 11</sup>. A  
30 model recently suggested biomass turnover rates on the order of thousands of years in the marine  
31 subsurface that are hypothesized to have an impact on global biogeochemical cycling over  
32 geological timescales<sup>4</sup>. Logistical sampling constraints, the complex sediment matrix composed  
33 of organic material and minerals, and low metabolic rates<sup>3, 4</sup>, have hindered directed testing of  
34 microbial activities at the molecular level in this environment. A better understanding of deep  
35 biosphere activities will help define the deep biosphere's role in global biogeochemical cycles<sup>12</sup>.

36 We optimized an mRNA extraction and amplification protocol for subseafloor sediment,  
37 and combined this with high-throughput sequencing to report the first dataset on microbial gene  
38 expression in the marine subsurface, demonstrating that despite the extremely low metabolic  
39 rates<sup>1, 4</sup>, mRNA-based investigations of the deep biosphere are possible and informative. We  
40 use the gene expression data to reconstruct active community metabolism and results support  
41 calculations<sup>1</sup> and models<sup>4</sup> of sub-seafloor microbial activities. The Peru Margin (Ocean Drilling  
42 Program Leg 201, Site 1229D) was analyzed because a wealth of biogeochemical data exists for  
43 this site <sup>e.g. 1, 4, 6, 9, 10</sup> that exhibits peaks of cell abundance, and profiles of sulfate and methane  
44 suggestive of microbial activity<sup>1</sup> (Figure 1).

45 Picogram quantities of total RNA were extracted from 25 grams of Peru Margin sediment  
46 from six depths (5, 30, 50, 70, 91, 159 mbsf), consistent with basal levels of microbial activity

47 predicted for this environment<sup>3,4</sup>. Illumina<sup>®</sup> sequencing of total cDNA produced over 1 billion  
48 reads, with 50% to 85% of reads mapping to open reading frames that were assigned a functional  
49 annotation (Table S1).

50 The dominance of transcripts from Firmicutes, Actinobacteria, Alphaproteobacteria, and  
51 Gammaproteobacteria (Fig. S1) is consistent with previous cultivation-based, metagenomic, and  
52 phylogenetic surveys from Peru Margin subsurface sediment<sup>1, 5, 13, 14</sup>, and suggests these to be  
53 some of the most active microbial groups. The abundance of gammaproteobacterial transcripts  
54 (Fig. S1) suggests that they are likely the most active microbial group in the deeper, anoxic,  
55 subseafloor sediment at this site. Fungal transcripts were also present in every sample ranging in  
56 representation from 3% at 70 mbsf to 20% at 5 mbsf. Archaea and Chloroflexi are present in  
57 noticeably low abundance, despite their previous detection at this site<sup>6, 13, 15</sup>, suggesting that our  
58 approach might miss organisms with lower mRNA expression levels. As such, interpretations of  
59 relative abundances should be treated cautiously<sup>16</sup>. Changes in pressure and temperature may  
60 have altered gene expression during sampling. However, low representation of heat shock  
61 proteins (a proxy for physiological stress response<sup>17</sup>) in protein coding reads ( $< 10^{-5}$ %) suggests  
62 the physiological state of most microbes was not significantly altered during sample retrieval and  
63 storage.

64 Dissimilatory sulfate reduction may represent a major form of microbial metabolism and  
65 energy production in the sub-seafloor<sup>1, 2, 18</sup> and is indicated by porewater sulfate concentrations at  
66 Site 1229<sup>1</sup> (Fig. 1). Representation of *Dsr* transcripts was highest in sediment with sulfate  
67 profiles suggestive of biogenic sulfate reduction (Fig. 1) and supports biogeochemical evidence  
68 for sulfate reduction at this site<sup>1, 4</sup>. Surprisingly, transcripts coding for dissimilatory nitrate  
69 reductases (*Nar*) were represented throughout the sediment column, despite no measureable

70 nitrate. The origin of nitrate as a substrate in this sediment is unknown, but could potentially be  
71 produced as a by-product of anaerobic ammonium oxidation. Once produced, nitrate would  
72 likely not accumulate to measurable concentrations given the higher free energy yield of nitrate  
73 as electron acceptor compared to the dominant electron acceptors in this environment, sulfate  
74 and iron. Nitrate reduction appears to be performed predominantly by Alphaproteobacteria and  
75 Betaproteobacteria at most depths (Fig. 1) and the resulting nitrite is likely reduced by Fungi,  
76 Gammaproteobacteria, and Firmicutes (Fig. S3). In contrast, Deltaproteobacteria and Firmicutes  
77 are the dominant groups expressing *Dsr* transcripts at 5 and 30 mbsf, and Gammaproteobacteria  
78 were the only group with detectable *Dsr* transcripts at deeper depths (Fig. 1). Expression of *Dsr*  
79 transcripts from a methanogenic lineage (Fig 1) in the deep biosphere supports the evidence that  
80 anaerobic oxidation of methane (AOM) may not be an obligate syntrophic process<sup>19</sup>.

81 Gene expression from methanogenic lineages was found, including Methanosarcinales,  
82 which contain the anaerobic methane-oxidizing group ANME-2<sup>20</sup> (Fig. S4). However, we did  
83 not detect any transcripts coding for methyl-coenzyme reductase M (*mcrA*), arguably the best  
84 diagnostic enzyme for AOM and methanogenesis. This could be explained by low levels of  
85 archaeal mRNA expression and a masking of *mcrA* gene expression by archaeal housekeeping  
86 genes. As a DNA-based study detected *mcrA* genes from this site<sup>21</sup>, this explanation seems  
87 likely. Consistent with DNA-based observations from other sites<sup>20</sup>, gene expression from  
88 methanogens was detected in the sulfate reduction zones (Fig. S4). Methylotrophic  
89 methanogenesis has been documented in shallow sediment sulfate reduction zones that contain  
90 non-competitive substrates such as trimethylamine<sup>22, 23</sup>. Our detection of trimethylamine  
91 methyltransferase transcripts from Methanosarcinales and Methanobacteriales (Fig S4) suggests  
92 that this process occurs in the deep seafloor and support previous suggestions of biogenic



93 methane at this site<sup>1</sup>. While Crenarchaeota have been suggested to be dominant at this site<sup>6, 13, 15</sup>,  
94 they are a minority contribution to the metatranscriptome (Fig S1) even with incorporating new,  
95 partially completed, single cell genomes from shallow sediments<sup>24</sup> (Table S2). One explanation  
96 is that Crenarchaeota may have relatively low levels of mRNA expression in the deep biosphere.

97 A model suggests turnover of microbial biomass in this environment<sup>4</sup>, but at the  
98 extremely low metabolic rates proposed it is unknown whether growth yield leads to cell division  
99 or to biomass turnover without division<sup>4, 25</sup>. Representation of transcripts involved in cell  
100 division (Table S3) increases at sulfate methane transition zones (SMTZs) where cell abundances  
101 increase by an order of magnitude ( $p = 0.03$ , Figs 1, S5). Our data suggest that the portion of the  
102 vegetative population that is actively dividing is largest in the SMTZs, and that observed peaks  
103 in cell counts at SMTZs are a result of *in situ* cell division. Cell division transcripts from all three  
104 domains of life strongly indicate a diversity of actively dividing cells in deeply buried sediment,  
105 including Fungi. The dominance of transcripts involved in amino acid metabolism (Fig. 2) and  
106 coding for peptidases (Fig. S6) support a recent model of amino acid turnover in the deep  
107 biosphere<sup>4</sup> and evidence for peptidase activity in shallow marine sediments<sup>24</sup>.

108 Microbial motility has been proposed for deep sediment<sup>5</sup>, however, calculations of mean  
109 metabolic rates suggest that flagellar motility may not be possible in the deep biosphere<sup>26</sup>. We  
110 detected expressed ORFs involved in flagellar, gliding, and twitching based motility (Table  
111 S3) up to 159 mbsf (Fig. 3) and the abundance of these categories decreases with decreasing  
112 sediment porosity ( $p = 0.01$ , Fig. 3), indicating that microbial motility is related to the space  
113 available for movement. The evidence for motility presented here implies that metabolic rates are  
114 not equal across all cells in the deep biosphere and that some cells may be significantly more

115 metabolically active than others. The offset in taxonomic assignment of motility reads (Fig. S7)  
116 relative to total mRNA reads (Fig. S1) is suggestive of such differences.

117 DNA repair may represent a mechanism by which microbes in the deep biosphere are  
118 able to cope with the slow degradation of DNA over geological timescales due to spontaneous  
119 chemical or radiolytic reactions in the subseafloor<sup>25, 26</sup>. The representation of DNA repair  
120 transcripts involved in nucleotide excision and mismatch repair (Table S3) increases linearly  
121 with sediment depth ( $p = 0.004$ , Fig. 3). This suggests DNA repair is a survival mechanism for  
122 microbial populations in ancient sediment and supports the suggestion that dormancy may not be  
123 a feasible survival strategy for the deep biosphere, because it does not completely arrest the slow  
124 degradation of DNA<sup>25, 26</sup>.

125 Fungal metabolic transcripts confirm previous suggestions of living fungi in the  
126 subseafloor<sup>9, 13, 27</sup>, and are the first direct evidence for active fungal metabolism in the deep  
127 biosphere. Five percent of transcripts involved in carbohydrate, amino acid, and lipid  
128 metabolism were assigned to Fungi, suggesting that Fungi play an overlooked role in organic  
129 carbon turnover in sub-seafloor sediment (Fig. 2). Fungal expression of transcripts coding for  
130 hydrolases involved in protein, carbohydrate, and lipid degradation (Fig. S6) indicates they  
131 degrade a variety of organic carbon substrates in deep subseafloor sediment.

132 Microbial expression of antibiotic defense mechanisms, polyketide synthases, and non-  
133 ribosomal proteins was detected (Fig. S8). Polyketide synthases and non-ribosomal proteins are  
134 involved in the biosynthesis of natural products (*e.g.* antibiotics, immunosuppressants,  
135 antifungals) of clinical and industrial importance. These findings warrant further investigation  
136 into potentially novel secondary metabolites produced by the deep biosphere, and support the

137 hypothesis that the deep biosphere may represent a “seed bank” of novel biotechnological and  
138 biomedical innovation<sup>28</sup>.

139 A comparison of the metatranscriptomic data to existing metagenomic datasets from this  
140 site<sup>13, 29</sup> reveals an increased representation of key metabolic and cell cycle functional genes in  
141 the metatranscriptome including those involved in DNA repair, DNA replication, transcription,  
142 amino acid biosynthesis, and lipid biosynthesis (Fig. 4). The significant difference between  
143 mRNA and metagenome samples with similar biogeochemical profiles (upper SMTZ and 50  
144 mbsf: 5/12 samples) suggests these to be some of the more active processes. Although not a  
145 primary group in the overall annotations, activity of Archaea in the deep biosphere is highlighted  
146 by archaeal ATPase and DNA polymerase transcripts that are overrepresented in the  
147 metatranscriptomes relative to metagenomes ( $p < 0.0005$ ). An analysis of similarity test  
148 (ANOSIM) indicates that the gene expression approach captures a significantly different picture  
149 of microbial activities compared to DNA based data ( $p=0.001$ , Fig. S9). As deep biosphere  
150 studies move forward, joint investigation of both nucleic acid pools are needed for full  
151 interpretation of metabolic activity and potential.

152 Metatranscriptomic analysis enables a refined view of deep biosphere activities.  
153 Microbial activity in deeply buried marine sediment is important because the collective activities  
154 of subsurface microbiota directly influences whether elements such as carbon are sequestered for  
155 millions of years in sediment or returned to the ocean, impacting food webs and climate<sup>12</sup>. Our  
156 data suggest the latter is mediated by diverse metabolic activities across all three domains of life  
157 in the sub-seafloor.

158

159 **METHODS SUMMARY**

160 **Sample collection.** Subsurface sediment samples from the continental shelf of Peru, Ocean  
161 Drilling Program (ODP) Site 1229D (77° 57.4590' W, 10° 58.5721' S), were obtained during  
162 ODP Leg 201 on March 6<sup>th</sup>, 2002.

163 **RNA extraction, purification, and amplification.** RNA was extracted from 25 g subseafloor  
164 sediment according to the protocol described by Orsi *et al*<sup>26</sup> using the FastRNA Pro Soil-Direct  
165 Kit<sup>®</sup> (MP Biomedicals, Solon, OH). In addition to the manufacturers instructions, physical and  
166 chemical adjustments to the sample were used to increase RNA yield and purity (see  
167 Supplemental Methods). DNA was removed using the Turbo DNA-free<sup>®</sup> kit (Life Technologies,  
168 Grand Island, NY), increasing the incubation time to 1 hour to ensure rigorous DNA removal.  
169 The MEGA-Clear<sup>®</sup> RNA Purification Kit (Life Technologies, Grand Island, NY) was used to  
170 further purify the RNA. Removal of contaminating DNA in RNA extracts was confirmed by  
171 the absence of visible amplification of SSU rRNA genes after 35 cycles of PCR using the RNA  
172 extracts as template. Total RNA was used as template for cDNA amplification using the Ovation  
173 RNA-Seq v2 System<sup>®</sup> (NuGEN technologies).

174 **Bioinformatic analyses.** Quality control was performed using FastQC  
175 (<http://www.bioinformatics.babraham.ac.uk/projects/fastqc/>). Read assembly and mapping were  
176 performed in CLC Genomics Workbench 5.0 (CLC Bio Inc.). The Rapid Analysis of Multiple  
177 Metagenomes with a Clustering and Annotation Pipeline (RAMMCAP) available through  
178 CAMERA (<http://camera.calit2.net/>) was used to annotate contigs against COG and Pfam  
179 databases. Heatmaps and statistical tests were performed in R (<http://www.r-project.org/>) using  
180 the vegan (<http://vegan.r-forge.r-project.org/>) and matR (metagenomics.anl.gov) packages.  
181 Taxonomic assignments of contigs were performed using PhymmBL<sup>30</sup> with addition of fungal

182 genomes available in the NCBI RefSeq and JGI databases and four partial single cell archaeal  
183 genomes from a shallow sediment site<sup>24</sup>.

184

185

## 186 REFERENCES

- 187 1. D'Hondt, S. *et al.* Distributions of microbial activities in deep subseafloor sediments.  
188 *Science* **306**, 2216-2221 (2004).
- 189 2. Schrenk, M. O., Huber, J. A., & Edwards, K. J. Microbial provinces in the subseafloor.  
190 *Ann Rev Mar Sci* **2**, 279-304 (2010).
- 191 3. Jorgensen, B. B. & D'Hondt, S. A starving majority deep beneath the seafloor. *Science*  
192 **314**, 932-934 (2006).
- 193 4. Lomstein, B. A., Langerhuus, A. T., D'Hondt, S., Jorgensen, B. B., & Spivack, A. J.  
194 Endospore abundance, microbial growth and necromass turnover in deep sub-seafloor  
195 sediment. *Nature* **484**, 101-104 (2012).
- 196 5. Parkes, J., Cragg, B., & Wellsbury, P. Recent studies on bacterial populations and  
197 processes in subseafloor sediments: A review. *Hydrogeol J* **8**, 11-28 (2000).
- 198 6. Biddle, J. F. *et al.* Heterotrophic Archaea dominate sedimentary subsurface ecosystems  
199 off Peru. *Proc Natl Acad Sci USA* **103**, 3846-3851 (2006).
- 200 7. Kallmeyer, J., Pockalny, R., Adhikari, R., Smith, D. C., & D'Hondt, S. Global  
201 distributions of microbial abundance and biomass in subseafloor sediment. *Proc Natl*  
202 *Acad Sci U S A* **109**, 16213-16216 (2012).
- 203 8. Whitman, W. B., Coleman, D. C., & Wiebe, W. J. Prokaryotes: The unseen majority.  
204 *Proc Natl Acad Sci U S A* **95**, 6578-6583 (1998).

- 205 9. Biddle, J. F., House, C. H., & J. E. Brenchley. Microbial stratification in deeply buried  
206 marine sediment reflects changes in sulfate/methane profiles. *Geobiology* **3**, 287-295  
207 (2005).
- 208 10. D'Hondt, S. *et al.* Subseafloor sedimentary life in the South Pacific Gyre. *Proc Natl*  
209 *Acad Sci U S A* **106**, 11651-11656 (2009).
- 210 11. D'Hondt, S., Rutherford, S., & Spivack, A. J. Metabolic activity of subsurface life in  
211 deep-sea sediments. *Science* **295**, 2067-2070 (2002).
- 212 12. Hinrichs, K. U. & Inagaki, F. Downsizing the deep biosphere. *Science* **338**, 204-205  
213 (2012).
- 214 13. Biddle, J. F., Fitz-Gibbon, S., Schuster, S. C., Brenchley, J. E., & House, C. H.  
215 Metagenomic signatures of the Peru Margin subseafloor biosphere show a genetically  
216 distinct environment. *Proc Natl Acad Sci USA* **105**, 10583-10588 (2008).
- 217 14. Teske, A. In: *Proceedings of the Ocean Drilling Program, Volume 201, Scientific Results.*  
218 B. B. Jørgensen *et al.*, Eds. (ODP, College Station, TX, 2006), Chapter 2, pp. 1–19  
219 ([http://www-odp.tamu.edu/publications/201\\_SR/120/120.htm](http://www-odp.tamu.edu/publications/201_SR/120/120.htm)).
- 220 15. Lipp, J. *et al.* Significant contribution of Archaea to extant biomass in marine subsurface  
221 sediments. *Nature* **454**, 991-994 (2008).
- 222 16. Moran, M. A. *et al.* Sizing up metatranscriptomics. *ISME J* **7**, 237-243 (2012).
- 223 17. Gao, H. *et al.* Global transcriptome analysis of the heat shock response of *Shewanella*  
224 *oneidensis*. *J Bacteriol* **22**:7766-7803 (2004).
- 225 18. Jørgensen, B. B., D'Hondt, S., & Miller, D. J. In: *Proceedings of the Ocean Drilling*  
226 *Program, Volume 201, Scientific Results*, (ODP, College Station, TX, 2006), pp. 1–45  
227 ([www-odp.tamu.edu/publications/201\\_SR/201sr.htm](http://www-odp.tamu.edu/publications/201_SR/201sr.htm)).

- 228 19. Milucka, J. *et al.* Zero valent sulphur is a key intermediate in marine methane oxidation.  
229 *Nature* **491**, 541-546 (2012).
- 230 20. Lever, M. Functional gene surveys from ocean drilling expeditions - a review and  
231 perspective. *FEMS Microbiol Eco* **84**, 1-23 (2013).
- 232 21. Webster, G., Parkes, R. J., Cragg, B. A., Newberry, C.J., Weightman, A. J., Fry, J. C.  
233 Prokaryotic community composition and biogeochemical processes in deep subseafloor  
234 sediments from the Peru Margin. *FEMS Microbiol Ecol* **58**, 65-85 (2006).
- 235 22. Oremland, R. S. & Polcin, S. Methanogenesis and Sulfate Reduction: Competitive and  
236 noncompetitive substrates in estuarine sediments. *Appl Environ Microbiol* **44**, 1270-1276  
237 (1982).
- 238 23. Valentine, D. L. Emerging topics in marine methane biogeochemistry. *Annu Rev Mar Sci*  
239 **3**:147-171 (2011).
- 240 24. Lloyd, K. *et al.* Predominant archaea in marine sediments degrade detrital proteins.  
241 *Nature* **496**, 215-218 (2013).
- 242 25. Jorgensen, B. B. Deep subseafloor microbial cells on physiological standby. *Proc Natl*  
243 *Acad Sci USA* **108**, 18193-18194 (2011).
- 244 26. Hoehler, T. M & Jorgensen, B. B. Microbial life under extreme energy limitation. *Nat*  
245 *Rev Microbiol* **11**, 83-94 (2013).
- 246 27. Orsi, W., Biddle, J., Edgcomb. Deep sequencing of subseafloor eukaryotic rRNA reveals  
247 active Fungi across multiple subsurface provinces. *PLoS ONE* **8**, e56335 (2013).
- 248 28. Parkes, R. J. & Wellsbury P. in *Microbial Diversity and Bioprospecting*. (ed Bull, A.T.)  
249 120-129 (ASM Press, 2004).
- 250 29. Martino, A. J. *et al.* Novel degenerate PCR method for whole-genome amplification

251 applied to Peru Margin (ODP Leg 201) subsurface samples. *Front Microbiol* **3**, 17  
252 (2012).

253 30. Brady, A. & Salzberg, S. L. Phymm and PhymmBL: Metagenomic phylogenetic  
254 classification with interpolated markov models. *Nature Methods* **6**, 673-676 (2009).

255 -

256 **Supplementary Information** is linked to the online version of the paper at  
257 [www.nature.com/nature](http://www.nature.com/nature).

258 **Acknowledgements** This work was fostered by a Center for Dark Energy Biosphere  
259 Investigations (CDEBI) grant OCE-0939564 to WO and a NSF IOS grant 1238801 to JFB. We  
260 thank Christopher House (Penn State U.) and Andreas Teske (UNC) for graciously providing  
261 samples. We also thank Mitchell Sogin and Richard Fox at the Josephine Bay Paul Center  
262 (Marine Biological Laboratory, Woods Hole, MA) for kindly providing access to computing  
263 resources. Edward Leadbetter (WHOI) and Steven Hallam (UBC) provided helpful comments on  
264 the manuscript, and we also thank Steven D'Hondt (URI) for helpful discussions on the deep  
265 biosphere. This is CDEBI contribution 137.

266 **Author Contributions** W.O. performed experiments, analyzed data, and wrote the paper; W.O.,  
267 J.B., and V.E. designed experiments and developed ideas. W.O. and G.C. developed analytical  
268 tools. All authors participated in data interpretation and provided editorial comments on the  
269 manuscript.

270 **Author Information** Data has been deposited in the NCBI Short Read Archive under accession  
271 number SRA058813 and in MG RAST ([metagenomics.anl.gov](http://metagenomics.anl.gov)) under accession numbers  
272 4515478.3, 4515477.3, 4515476.3, 4510337.3, 4510336.3, and 4510335.3. Reprints and  
273 permission information is available at [www.nature.com/reprints](http://www.nature.com/reprints). The authors declare no



274 competing interests. Correspondence and requests for materials should be addressed to W.O.  
275 (william.orsi@gmail.com).

276

277

278

## 279 **Figure and Table legends**

280

281 **Figure 1:** Biogeochemical and gene expression profiles of the deep biosphere from Peru Margin  
282 sediments, IODP site 1229D. **(a)** Cell abundance, sulfate concentrations, and methane  
283 concentrations, dotted lines indicate the SMTZs. Values were taken from the Ocean Drilling  
284 Program Janus Database (<http://www-odp.tamu.edu/database/>). **(b)** Proportion of cell division  
285 transcripts within the cluster of orthologous genes (COG) class D (cell cycle control/cell  
286 division/chromosome partitioning, n = 30.22 million reads), see Table S3 for description of cell  
287 division proteins. The proportion of **(c)** *Dsr* and **(d)** *Nar* transcripts relative to total transcripts  
288 involved in energy production (COG class C, n = 92.33 million reads). See Figure S2 for  
289 number of sequences and ORFs used in each comparison, and *E*-values for hits in the COG  
290 database.

291

292 **Figure 2:** The proportion of reads mapping to ORFs assigned to amino acid, lipid, and  
293 carbohydrate metabolism (eleven most dominant taxa shown). Note the relative abundance of  
294 amino acid metabolism (both anabolic and catabolic) relative to lipid and carbohydrate  
295 metabolism across all depths. See Figure S2 for the number of sequences and ORFs used in each  
296 comparison, and *E*-values for hits in the COG database.

297

298 **Figure 3:** Transcripts involved in cell motility and DNA repair. **(a)** The percentage of reads  
299 mapping to ORFs coding for proteins involved in different modes of cellular motility (see Table  
300 S3 for descriptions). **(b)** A correlation of cell motility transcripts versus sediment porosity ( $R^2 =$   
301 0.8,  $p = 0.01$ ) and 95% prediction interval (red dotted lines). **(c)** The percentage of reads  
302 mapping to ORFs involved in DNA repair (only eleven most dominant taxa are shown, see Table  
303 S3 for descriptions). **(d)** A correlation of DNA repair transcripts versus sediment depth ( $R^2 = 0.9,$   
304  $p = 0.004$ ) and 95% prediction interval (red dotted lines). See Figure S2 for the number of  
305 sequences and ORFs used in each comparison and *E*-values for ORF hits in COG database.

306

307 **Figure 4:** A comparison of gene expression data to existing metagenomic studies<sup>13, 29</sup> from  
308 IODP site 1229. Functional genes significantly (Kruskal-Wallis test,  $p < 0.0005$ )  
309 overrepresented in the metatranscriptomic samples relative to metagenomic data include DNA  
310 repair and replication transcripts, RNA polymerase, and archaeal ATPase and DNA polymerase  
311 transcripts. The dendrogram represents a UPGMA hierarchical clustering analysis (Manhattan  
312 distance) of significantly overrepresented mRNA transcripts, note the complete separation of  
313 mRNA samples from DNA samples.

314

## 315 **Methods**

316 **Sample collection and storage** Subsurface sediment samples from the continental shelf of Peru,  
317 Ocean Drilling Program (ODP) Site 1229D (77° 57.4590' W, 10° 58.5721' S), were obtained  
318 during ODP Leg 201 on March 6<sup>th</sup>, 2002. Careful precautions were taken during sampling to  
319 avoid contamination during the sampling process. For IODP cores, contamination tests were  
320 performed using Perfluorocarbon tracers and fluorescent microspheres (for more information see

321 [http://www-odp.tamu.edu/publications/201\\_IR](http://www-odp.tamu.edu/publications/201_IR)). Sediment samples were immediately frozen at -  
322 80 °C after sampling and stored at -80 °C until used for mRNA extractions in this study (10 year  
323 storage time at -80 °C).

324 **RNA extraction and purification** Extraction of subseafloor RNA was performed according to  
325 the protocol of Orsi *et al* <sup>26</sup>. To summarize, RNA was extracted from 25 grams of sediment  
326 using the FastRNA Pro Soil-Direct Kit<sup>®</sup> (MP Biomedicals, Solon, OH). It was necessary to scale  
327 up the volume of sediment that is typically extracted with the kit (~0.5 grams) due to the low  
328 biomass inherent to marine subsurface samples. All tubes, tips, and disposables used were  
329 certified RNase free and all extraction procedures were performed in a laminar flow hood to  
330 reduce aerosol contamination by bacterial and fungal cells/spores. Five 15ml Lysing Matrix E<sup>®</sup>  
331 tubes (MP Biomedicals, Solon, OH) were filled with 5 g sediment and 5 ml of Soil Lysis  
332 Solution<sup>®</sup> (MP Biomedicals, Solon, OH). Tubes were vortexed to suspend the sediment and Soil  
333 Lysis Solution<sup>®</sup> was added to the tube leaving 1 ml of headspace. Tubes were then homogenized  
334 for 60 seconds on the FastPrep-24 homogenizer<sup>®</sup> (MP Biomedicals, Solon, OH) with a setting of  
335 4.5. Contents were pooled into two 50ml tubes and centrifuged for 30 minutes at 4,000 RPM  
336 (3220 x g) at room temperature (RT). Supernatants were combined in a new 50ml tube and 1/10  
337 volume of 2M Sodium Acetate (pH 4.0) was added. An equal volume of phenol-chloroform (pH  
338 6.5) was added and vortexed for 30 seconds, incubated for 5 minutes at room temperature, and  
339 spun at 4000 RPM (3220 x g) for 20 minutes at 4 °C. The aqueous phase was transferred to a  
340 new 50ml tube. Nucleic acids were precipitated by adding 2.5 and 1/10 volumes 100% ethanol  
341 and 3M Sodium Acetate, respectively, and incubating overnight at -80 °C. The next day, tubes  
342 were spun at 4000 RPM (3220 x g) for 60 minutes at 4 °C and the supernatant removed. Pellets  
343 were washed with 70% ethanol, spun for 15 minutes at 4 °C, and air-dried. Dried pellets were

344 resuspended with 0.25 ml RNase-free sterile water and combined into a new 1.5ml tube. 1/10  
345 volume of 2M Sodium Acetate (pH 4.0) and an equal volume of phenol:chloroform (pH 6.5)  
346 were added, vortexed for 1 minute, and incubated for 5 minutes at RT. This was necessary to  
347 remove residual organic material (*i.e.* humic acids) resulting from the rather large  
348 pellet/precipitate. After centrifuging at 14,000 RPM (20,817 x g) for 10 minutes at 4 °C, the top  
349 phase was removed into a new 1.5ml tube. 0.7 volumes of 100% isopropanol was added and  
350 incubated for 1 hour at -20 °C (to precipitate nucleic acids). Tubes were then centrifuged for 20  
351 minutes at 14,000 (20,817 x g) RPM at 4 °C and the supernatant removed. Pellets were washed  
352 with 70% ethanol and centrifuged at 14,000 RPM (20,817 x g) for 5 minutes at 4 °C. After  
353 removing ethanol and air-drying, pellets were resuspended in 0.2 ml of RNase free sterile water.  
354 DNA was removed using the Turbo DNA-free<sup>®</sup> kit (Life Technologies, Grand Island, NY),  
355 increasing the incubation time to 1 hour to ensure rigorous DNA removal. After this step,  
356 samples were taken through the protocol supplied with the FastRNA Pro Soil-Direct kit<sup>®</sup> to the  
357 end (starting at the RNA Matrix<sup>®</sup> and RNA Slurry<sup>®</sup> addition step), including the column  
358 purification step to remove residual humic acids (see FastRNA Pro Soil-Direct Kit<sup>®</sup> manual).  
359 Extraction blanks were performed (adding sterile water instead of sample) to ensure that  
360 aerosolized contaminants did not enter sample and reagent tubes during the extraction process.  
361 Absence of DNA and RNA contamination was confirmed by no visible amplification of small  
362 subunit (SSU) rRNA and rRNA genes from extraction blanks after 35 cycles of PCR and RT-  
363 PCR.

364           After RNA extraction, used the MEGA-Clear<sup>®</sup> RNA Purification Kit (Life Technologies,  
365 Grand Island, NY) to purify the RNA. This kit removes short RNA fragments (mostly produced  
366 during the extraction protocol) and residual inhibitors (*i.e.* humics). We followed the protocol all

367 the way through the optional precipitation/concentration step, resuspending the RNA pellet in 10  
368 microliters of RNase free sterile water. Prior to cDNA amplification, the removal of  
369 contaminating DNA in RNA extracts was confirmed by the absence of visible amplification of  
370 SSU rRNA genes after 35 cycles of PCR using the RNA extracts as template.

371 **cDNA amplification and Illumina sequencing** Five microliters of purified RNA was used as  
372 template for whole cDNA amplification using the Ovation RNA-Seq v2 System<sup>®</sup> (NuGEN  
373 technologies, <http://www.nugeninc.com/nugen/index.cfm/products/cs/ngs/rna-seq-v2/>). We  
374 followed the manufacturers instructions for cDNA amplification, and the resulting quantity of  
375 cDNA was checked on a Nanodrop (Thermo Scientific) and Fluorometer (Qubit 2.0, Life  
376 Technologies). Quality of the amplified cDNA was checked on a Bioanalyzer (Agilent  
377 Biotechnologies) prior to Illumina<sup>®</sup> sequencing. Illumina<sup>®</sup> library preparation and paired-end  
378 sequencing was performed at the University of Delaware Sequencing and Genotyping Center  
379 (Delaware Biotechnology Institute, Newark DE).

380 **Quality control and assembly** Quality control of the dataset was performed using FastQC  
381 (<http://www.bioinformatics.babraham.ac.uk/projects/fastqc/>), with a quality score cutoff of 28.  
382 Approximately 1 billion paired-end reads that passed quality control were imported into CLC  
383 Genomics Workbench 5.0<sup>®</sup> (CLC Bio Inc.) and assembled using the paired-end Illumina  
384 assembler. Contigs were assembled over a range of kmer sizes (20, 50, 60, 64) with a minimum  
385 contig size cutoff of 300 nucleotides. The kmer size of 50 resulted in the highest number of  
386 contigs and these contigs were chosen for use in downstream analyses. To reduce the formation  
387 of chimeric assemblies, we used a paired-end sequencing approach and performed assemblies  
388 without scaffolding. Reads were mapped onto the contigs using the read mapping option in CLC  
389 Genomics Workbench to retain information on relative abundance of contigs.

390 **Functional annotation of contigs** Contigs were submitted to CAMERA (Community  
391 Cyberinfrastructure for Advanced Microbial Ecology Research and Analysis,  
392 <http://camera.calit2.net/>) and assigned to clusters of orthologous gene (COG) families, gene  
393 ontologies (GO), and protein families (Pfam), using the Rapid Analysis of Multiple  
394 Metagenomes with a Clustering and Annotation Pipeline (RAMMCAP) using the 6 reading  
395 frame translation option for open reading frame (ORF) prediction and BLASTn for rRNA  
396 identifications. The cutoff criterion *E*-value of  $10^{-5}$  was used for BLASTx searches against the  
397 COG, Pfam, and TIGRfam databases. For identification of bacterial and archaeal ORFs, the  
398 RAMMCAP analyses were performed using the bacterial and archaeal genetic code (-t 11 in  
399 advanced options). For identification of fungal ORFs, additional RAMMCAP analyses were  
400 performed using the standard genetic code for eukaryotes and the alternative yeast genetic code  
401 (-t 1 and -t 12 in advanced options). For comparative analysis of the metatranscriptomes to  
402 existing metagenomes from ODP Site 1229D we submitted the metatranscriptomes to MG-  
403 RAST ([metagenomics.anl.gov](http://metagenomics.anl.gov)), which were annotated according to the standard bioinformatics  
404 pipeline (<http://blog.metagenomics.anl.gov/mg-rast-for-the-impatient-readme-1st/>).

405 **Taxonomic annotation of contigs** Contigs were assigned to high-level taxonomic groups (Class  
406 level and above) using PhymmBL<sup>30</sup>. In addition to the default interpolated markov model  
407 (IMM) database (that contains only bacterial and archaeal genomes), all fungal genomes  
408 available in the NCBI RefSeq database and JGI database, along with several representative  
409 protistan and plant genomes were added to the IMM database (using the customGenomicData.pl  
410 script available with the PhymmBL download) to facilitate identification of eukaryotic contigs.  
411 Cutoffs for annotation accuracy were chosen based on the default recommendations. Taxonomic  
412 identifications of contigs made using PhymmBL<sup>30</sup> were integrated with the functional

413 annotations from CAMERA (BLASTx searches against the COG database and HMMer searches  
414 against Pfam database) and the read mapping information from assemblies. This was done using  
415 several custom PERL scripts that are available from the authors upon request.

416 **Statistical analyses** Analyses of overexpression of expressed genes relative to metagenome  
417 samples was performed using the R statistical package (<http://www.r-project.org/>), with the MG-  
418 RAST matR library ([metagenomics.anl.gov](http://metagenomics.anl.gov)). To maintain abundance information, assembled  
419 contig sequences from each sample were uploaded to MG RAST with the read mapping  
420 abundance added to the fasta headers as specified on the MG RAST website. Statistically  
421 significant differences in overexpressed functional genes relative to genes detected in  
422 metagenomes were determined by a Kruskal-Wallis test with a p value cutoff of 0.0005. All  
423 rRNA reads were removed from both metagenomic and metatranscriptomic datasets prior to  
424 comparison. Data were normalized in MG RAST with a log based transformation:

$$425 \quad Y_{s,i} = \log_2 (X_{s,i} + 1)$$

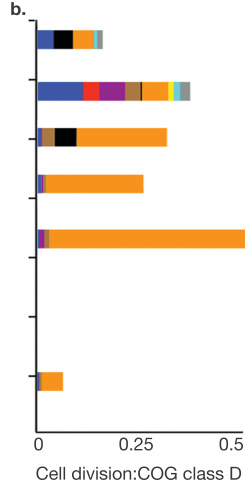
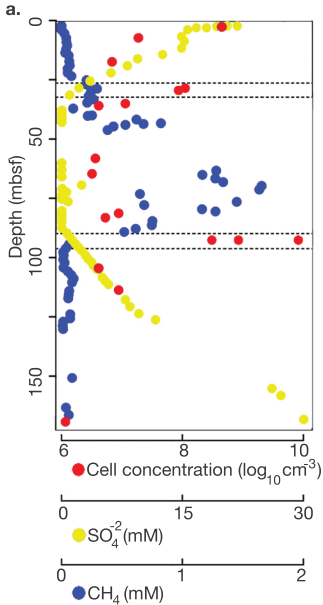
426 Where  $X_{s,i}$  represents an abundance measure ( $i$ ) in sample ( $s$ ). Log transformed counts from each  
427 sample were then standardized (data centering) according to the following equation:

$$428 \quad Z_{s,i} = [(Y_{s,i} - Y_s) / \sigma_s]$$

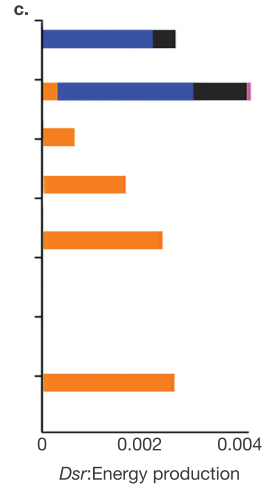
429 Where  $Z_{s,i}$  is the standardized abundance of an individual measure  $Y_{s,i}$  (log transformed from  
430 previous equation). From each log transformed measure of ( $i$ ) in sample ( $s$ ), the mean of all  
431 transformed values ( $Y_s$ ) is subtracted and the difference is divided by the standard deviation ( $\sigma_s$ )  
432 of all log-transformed values for the given sample. After log transformation and standardization,  
433 the values for the functional categories within each sample were scaled from 0 (minimum value  
434 of all samples) to 1 (maximum value of all samples), which is a uniform scaling that does not  
435 affect the relative differences of values within a single sample or between 2 or more samples.

436 This procedure places the value of functional categories (*i.e.* COG categories) from each sample  
437 on a scale from 0 to 1 and was used to produce figures (*i.e.* heatmaps or principal component  
438 analysis) where the abundance range is on a scale from 0 to 1 (*i.e.* Figure 4). Normalized data  
439 that passed the Kruskal-Wallis test (p value cutoff criterion 0.0005) were used as input for  
440 heatmap presentation, UPGMA hierarchical clustering, and principal component analysis in R,  
441 using the matR package (metagenomics.anl.gov). Analysis of similarity (ANOSIM) analyses  
442 were performed on the normalized data in R, using the vegan package ([http://vegan.r-forge.r-](http://vegan.r-forge.r-project.org/)  
443 [project.org/](http://vegan.r-forge.r-project.org/)). ANOSIM was performed with 999 permutations using a Bray-Curtis distance  
444 metric. Correlations of gene expression data with geochemical and geophysical metadata were  
445 performed using the lm and predict commands in R, which are used to fit linear models to  
446 relationships between two different variables. The data for these analyses were normalized in  
447 the same fashion as Figures 1, 2, 3, S3, S4, S5, S6 and S8 (*i.e.* the relative abundance, per sample,  
448 of transcripts mapping to ORFs that were annotated to each functional COG category).

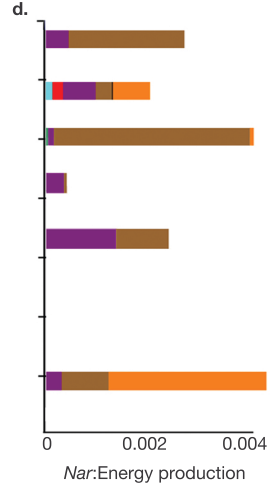




■ Crenarchaeota  
■ Actinobacteria  
■ Synergistes



■ Alphaproteobacteria  
■ Betaproteobacteria  
■ Methanomicrobiales



■ Deltaproteobacteria  
■ Gammaproteobacteria  
■ Euryarchaeota  
■ Firmicutes

